Rotational dispersion of active Brownian particles in plane Poiseuille flow

Zhiwei Peng†

Department of Chemical and Materials Engineering, University of Alberta, Edmonton, Alberta T6G 1H9, Canada

(Received xx; revised xx; accepted xx)

The transport of self-propelled particles and microorganisms in the presence of fluid flows and geometric confinement is important for the understanding of many biological and engineering processes, from the infection by motile bacteria to the formation of biofilms and the delivery of medical cargo. In plane Poiseuille flow, active Brownian particles (ABPs) are shown to exhibit intriguing dynamics including boundary accumulation, upstream swimming, and non-monotonic dependence of longitudinal dispersion on flow strength. Compared to the transport phenomena in position space, a theoretical understanding of the long-time orientational dynamics of active particles in spatially inhomogeneous flow remains lacking. In this work, we develop a generalized Taylor dispersion theory to analyze the long-time orientational transport of ABPs in plane Poiseuille flow. Our theory reveals that at long times the net orientational distribution satisfies an effective advection diffusion equation in orientation space. This model allows us to define an average angular drift and an effective rotational dispersion coefficient. For passive Brownian particles, we derive an exact solution to the rotational dispersion coefficient. Similar to the classical longitudinal Taylor dispersion of Brownian particles, we show that in strong flow the rotational dispersion coefficient has a quadratic scaling with the characteristic flow speed. For ABPs with finite swim speeds, we show that the rotational dispersion coefficient exhibits a non-monotonic dependence on the flow strength. Asymptotic analysis in the weak-swimming limit shows that compared to passive particles, activity can reduce the dispersion coefficient. The rotational GTD theory is validated against Brownian dynamics simulations. Our results show that the coupling between flow-induced rotations, confinement, activity, and Brownian diffusion can give rise to nontrivial transport dynamics in orientation space.

Key words: active matter, colloids, dispersion

1. Introduction

Transport and mixing of micron-sized particles in the presence of fluid flows and geometric confinement are important for various biological and industrial processes. At low Reynolds number, the coupling between spatially inhomogeneous fluid advection and Brownian motion often leads to enhanced mixing. The prototypical example of such an effect is the shear-enhanced longitudinal dispersion of a Brownian particle in Poiseuille flow through a channel (Taylor 1953), which is often refered to as Taylor dispersion. Brownian motion in the transverse direction of the channel allows the particle

† Email address for correspondence: zhiwei.peng@ualberta.ca

to sample different streamlines. As a result, the particle experiences a variation in its longitudinal advection as it migrates in the transverse direction. At long times, the interaction between transverse diffusion and longitudinal advection gives rise to enhanced longitudinal dispersion. Due to the prevalence of flow-induced dispersion, a generalized Taylor dispersion (GTD) theory was developed and has become an important paradigm for the understanding of a multitude of transport phenomena involving Brownian particles (Frankel & Brenner 1989; Brenner & Edwards 1993).

In recent decades, GTD has been further developed to accommodate the transport dynamics of motile microswimmers and particles such as gyrotactic microorganisms (Hill & Bees 2002; Manela & Frankel 2003; Bees & Croze 2010; Bearon *et al.* 2012), run-and-tumble particles (Bearon 2003), and active Brownian particles (Alonso-Matilla *et al.* 2019; Jiang & Chen 2019; Peng & Brady 2020). An active Brownian particle (ABP) self-propels with a constant swim speed U_s in a body-fixed direction $\boldsymbol{q}$ ($\boldsymbol{q}\cdot\boldsymbol{q}=1$). The swimming direction $\boldsymbol{q}$ randomizes over time due to rotational Brownian motion with a diffusivity D_R. When placed in planar Poiseuille flow, ABPs are shown to exhibit a non-monotonic dispersion behavior. In the weak flow limit, the dispersion coefficient is given by the sum of the bare translational diffusivity D_T and the swim diffusivity. When the flow speed is much larger than the swim speed, activity is obscured and the passive Taylor dispersion coefficient is obtained. As shown by Peng & Brady (2020), the dispersion coefficient as a function of the flow speed decreases for weak flow before it increases to meet the passive result in the strong flow limit. The minimum is obtained when the flow speed is comparable to the swim speed.

Compared to transport in position space, the long-time orientational transport of ABPs in planar Poiseuille flow remains poorly understood. In unbounded linear flows, Leahy *et al.* (2013, 2015) showed that axisymmetric particles exhibit enhanced rotational dispersion. Because the flow field is linear, the rotational dispersion does not depend on the activity (see section 2.2). In an earlier work (Peng 2024), we developed a GTD theory that describes the long-time orientational transport of an axisymmetric particle in unbounded linear flows. Here, we extend this theory to study the long-time orientational transport of ABPs in planar Poiseuille flow. For unbounded linear flows, one only needs to consider the orientational degree of freedom. In planar Poiseuille flow, both the position and orientation of the ABP need to be considered.

In this work, we show that ABPs exhibit a non-monotonic dispersion behavior in orientation space. For passive Brownian particles ($U_s = 0$), a closed-form analytic expression for the dispersion coefficient is obtained. Similar to the classical Taylor dispersion of Brownian particles in position space, the rotational dispersion coefficient has a quadratic scaling with the flow speed in the strong flow limit. Compared to the rotational dispersion of passive particles, active particles exhibit reduced dispersion. Using asymptotic analysis, we show that this swim-induced hindrance occurs at $O(Pe_s^2)$, where $Pe_s = U_s H/D_T$ with H being the half-width of the channel. The results from our continuum theory agree with those obtained from Brownian dynamics (BD) simulation that resolves the Langevin equations of motion.

This paper is organized as follows. In section 2, starting from the Smoluchowski equation we derive a GTD theory that describes the long-time orientational dynamics of an ABP in a generic flow field. We then specialize the equations for the case of a planar Poiseuille flow. We show that the average angular drift velocity vanishes. In section 3.1, an asymptotic solution in the weak-swimming limit is developed. We show that activity can reduce the long-time dispersion. We discuss the dispersion behavior for finite swim speeds in section 3.2 and compare the numerical solutions of the macrotransport equations with

those obtained from BD. The effect of particle shape on the long-time dispersion is considered in section 3.3. Lastly, we conclude in section 4.

2. Problem formulation

2.1. *The Smoluchowski equation*

We consider a dilute suspension of active Brownian particles (ABPs) in a generic background flow in two dimensions. The particles are assumed spherical and their size are negligible compared to the characteristic length of the flow. In a dilute suspension, we need only consider the dynamics and transport of a single active particle. The configuration of the particle is described by its position vector $\boldsymbol{x}$ and its unit orientation vector $\boldsymbol{q}$ ($\boldsymbol{q}\cdot\boldsymbol{q}=1$). Because the particle undergoes stochastic motion, we adopt a statistical mechanical description of its phase-space dynamics by defining the probability density function $P(\boldsymbol{x},\boldsymbol{q},t)$, where t is the time variable. The probability density function is governed by the Smoluchowski equation,

$$\frac{\partial P}{\partial t}+\boldsymbol{\nabla}\cdot\boldsymbol{j}_T+\boldsymbol{\nabla}_R\cdot\boldsymbol{j}_R=0, \tag{2.1}$$

where the translational and rotational fluxes are, respectively,

$$\boldsymbol{j}_T=U_s\boldsymbol{q}P+\boldsymbol{u}_fP-D_T\boldsymbol{\nabla}P, \tag{2.2a}$$

$$\boldsymbol{j}_R=\boldsymbol{\Omega}P-D_R\boldsymbol{\nabla}_RP. \tag{2.2b}$$

In (2.2a), the ABP is advected by its own swim speed U_s in the direction $\boldsymbol{q}$, the background flow velocity $\boldsymbol{u}_f$, and Brownian motion with diffusivity D_T. Similarly, in (2.2b), the ABP rotates due to the background flow and the rotational Brownian motion with diffusivity D_R. The angular velocity due to the flow $\boldsymbol{\Omega}=\boldsymbol{\omega}/2$ with $\boldsymbol{\omega}=\boldsymbol{\nabla}\times\boldsymbol{u}_f$ being the vorticity pseudovector. No-flux boundary condition is assumed to hold at any solid boundaries: $\boldsymbol{n}\cdot\boldsymbol{j}_T=0$, where $\boldsymbol{n}$ is a unit normal vector at the boundary. In (2.2b), $\boldsymbol{\nabla}_R=\boldsymbol{q}\times\frac{\partial}{\partial\boldsymbol{q}}$ is the gradient operator in orientation space (Brenner & Condiff 1974; Doi & Edwards 1988).

Integrating over the position space variable, we define the net orientational distribution as

$$\Psi(\boldsymbol{q},t)=\int P(\boldsymbol{x},\boldsymbol{q},t)\mathrm{d}\boldsymbol{x}. \tag{2.3}$$

From (2.1) and (2.2), we have

$$\frac{\partial\Psi}{\partial t}+\boldsymbol{\nabla}_R\cdot\left(\int\boldsymbol{\Omega}P\mathrm{d}\boldsymbol{x}-D_R\boldsymbol{\nabla}_R\Psi\right)=0, \tag{2.4}$$

where we have used the no-flux condition and assumed that at infinity the probability density decays to zero sufficiently fast. Because $\boldsymbol{\Omega}$ is a function of $\boldsymbol{x}$, the resulting equation (2.4) is not closed for Ψ. In general, one needs to calculate P before the integral can be carried out.

2.2. *A generalized Taylor dispersion theory*

In two dimensions, we parametrize $\boldsymbol{q}$ using the orientation angle ϕ such that $\boldsymbol{q}=\cos\phi\boldsymbol{e}_x+\sin\phi\boldsymbol{e}_y$, where $\phi\in[0,2\pi)$. Here, $\boldsymbol{e}_x$ and $\boldsymbol{e}_y$ are unit basis vectors of the Cartesian frame (x,y). With this, we write (2.4) as

$$\frac{\partial\Psi}{\partial t}+\frac{\partial}{\partial\phi}\left(\int\Omega P\mathrm{d}\boldsymbol{x}-D_R\frac{\partial\Psi}{\partial\phi}\right)=0, \tag{2.5}$$

where $\boldsymbol{\Omega} = \Omega \boldsymbol{e}_z$ and $\boldsymbol{e}_z = \boldsymbol{e}_x \times \boldsymbol{e}_y$. In the following, we treat the rotational dispersion of ABPs in Fourier space (Barakat & Takatori 2023; Peng 2024). To this end, we first define the unbounded angular coordinate as $\varphi = 2\pi j + \phi$, where $j \in \mathbb{Z}$ and ϕ is the bounded or local orientation angle. In other words, one may identify the cell index j as the global coordinate. We introduce the semidiscrete Fourier transform (Trefethen 2000)

$$\hat{f}(k) = 2\pi \sum_{j=-\infty}^{\infty} e^{-ikj2\pi} f_j, \tag{2.6}$$

where k is the wavenumber, and i ($i^2 = -1$) is the imaginary unit. With this definition, the global version of (2.5) in Fourier space may be written as

$$\frac{\partial \hat{\Psi}}{\partial t} + \left(ik + \frac{\partial}{\partial \phi} \right) \left[\int \Omega \hat{P} \mathrm{d}\boldsymbol{x} - D_R \left(ik + \frac{\partial}{\partial \phi} \right) \hat{\Psi} \right] = 0. \tag{2.7}$$

To reduce the above equation into a more familiar form, we first define the structure function $\hat{G}(\boldsymbol{x}, \phi, k, t)$ such that

$$\hat{P}(\boldsymbol{x}, \phi, k, t) = \left\langle \hat{\Psi} \right\rangle (k, t) \hat{G}(\boldsymbol{x}, \phi, k, t). \tag{2.8}$$

Invoking (2.8) and the periodic boundary condition on ϕ (Barakat & Takatori 2023; Peng 2024), we obtain

$$\frac{\partial \left\langle \hat{\Psi} \right\rangle}{\partial t} + ik \left\langle \int \Omega \hat{G} \mathrm{d}\boldsymbol{x} \right\rangle \left\langle \hat{\Psi} \right\rangle + k^2 D_R \left\langle \hat{\Psi} \right\rangle = 0, \tag{2.9}$$

where we have taken an average over the local cell: $\langle (\cdot) \rangle = (1/2\pi) \int_0^{2\pi} (\cdot) \mathrm{d}\phi$. Taking a small wavenumber expansion,

$$\hat{G}(\boldsymbol{x}, \phi, k, t) = g(\boldsymbol{x}, \phi, t) + ikb(\boldsymbol{x}, \phi, t) + O(k^2), \tag{2.10}$$

we obtain

$$\frac{\partial \left\langle \hat{\Psi} \right\rangle}{\partial t} + ik\Omega^{\mathrm{eff}} \left\langle \hat{\Psi} \right\rangle + k^2 D_R^{\mathrm{eff}} \left\langle \hat{\Psi} \right\rangle = 0, \tag{2.11}$$

where the average angular drift and effective dispersion coefficient are, respectively, given by

$$\Omega^{\mathrm{eff}} = \left\langle \int \Omega g \mathrm{d}\boldsymbol{x} \right\rangle, \quad \text{and} \quad D_R^{\mathrm{eff}} = D_R - \left\langle \int \Omega b \mathrm{d}\boldsymbol{x} \right\rangle. \tag{2.12}$$

We note that (2.11) is a long-time effective advection-diffusion equation written in Fourier space with the transport coefficients given in (2.12). In the following, we refer to g as the average field and b as the displacement field.

To calculate the transport coefficients, we need a set of equations for g and b. Subtracting (2.9) multiplied by $\hat{G}$ from the Fourier-transformed version of (2.1), we obtain

$$\begin{aligned} &\frac{\partial \hat{G}}{\partial t} + \boldsymbol{\nabla} \cdot \left(U_s \boldsymbol{q} \hat{G} + \boldsymbol{u}_f \hat{G} - D_T \boldsymbol{\nabla} \hat{G} \right) + ik \left(\Omega - \left\langle \int \Omega \hat{G} \mathrm{d}\boldsymbol{x} \right\rangle \right) \hat{G} \\ &- 2ikD_R \frac{\partial \hat{G}}{\partial \phi} + \frac{\partial}{\partial \phi} \left(\Omega \hat{G} - D_R \frac{\partial \hat{G}}{\partial \phi} \right) = 0. \end{aligned} \tag{2.13}$$

In the following, we focus on the steady state solution and time dependence will be

dropped. Inserting the expansion (2.10) into (2.13), we obtain at $O(1)$

$$\boldsymbol{\nabla}\cdot(U_s\boldsymbol{q}g+\boldsymbol{u}_f g-D_T\boldsymbol{\nabla}g)+\frac{\partial}{\partial\phi}\left(\Omega g-D_R\frac{\partial g}{\partial\phi}\right)=0. \tag{2.14}$$

The conservation condition is $\left\langle\int g\mathrm{d}\boldsymbol{x}\right\rangle=1$. At $O(k)$, we have

$$\boldsymbol{\nabla}\cdot(U_s\boldsymbol{q}b+\boldsymbol{u}_f b-D_T\boldsymbol{\nabla}b)+\frac{\partial}{\partial\phi}\left(\Omega b-D_R\frac{\partial b}{\partial\phi}\right)=\left(\Omega^{\mathrm{eff}}-\Omega\right)g+2D_R\frac{\partial g}{\partial\phi}, \tag{2.15}$$

and $\left\langle\int b\mathrm{d}\boldsymbol{x}\right\rangle=0$.

We note that the macrotransport equations (2.14) and (2.15) describe the long-time effective dynamics of an ABP in a generic flow field. For an unbounded linear flow, the angular velocity Ω is spatially homogeneous. In this case, we may define $\tilde{g}(\phi)=\int g(\boldsymbol{x},\phi)\mathrm{d}\boldsymbol{x}$, $\tilde{b}(\phi)=\int b(\boldsymbol{x},\phi)\mathrm{d}\boldsymbol{x}$, and obtain

$$\frac{\partial}{\partial\phi}\left(\Omega\tilde{g}-D_R\frac{\partial\tilde{g}}{\partial\phi}\right)=0, \tag{2.16a}$$

$$\frac{\partial}{\partial\phi}\left(\Omega\tilde{b}-D_R\frac{\partial\tilde{b}}{\partial\phi}\right)=\left(\Omega^{\mathrm{eff}}-\Omega\right)\tilde{g}+2D_R\frac{\partial\tilde{g}}{\partial\phi}. \tag{2.16b}$$

Equation (2.16) is obtained by Peng (2024) and used to study the long-time orientational dynamics of a spheroidal particle in simple shear and extensional flows. Because the flow field is linear, the swimming motion does not play a role in the long-time orientational dynamics. However, in spatially inhomogeneous flows, the swimming motion affects the long-time orientational dynamics.

2.3. *The case of a plane Poiseuille flow*

Consider a plane Poiseuille flow between two parallel plates with a separation distance $2H$. The channel walls are located at $y=\pm H$ and x is taken as the longitudinal coordinate. With this definition, the velocity field is given by

$$\boldsymbol{u}_f=U_f\left(1-\frac{y^2}{H^2}\right)\boldsymbol{e}_x, \tag{2.17}$$

where U_f is the flow speed at the channel centerline ($y=0$). The average field equation (2.14) reduces to

$$\frac{\partial}{\partial y}\left(U_s\sin\phi\, g-D_T\frac{\partial g}{\partial y}\right)+\frac{\partial}{\partial\phi}\left(\Omega g-D_R\frac{\partial g}{\partial\phi}\right)=0, \tag{2.18}$$

where g is invariant in x, $g=g(y,\phi)$. Similarly, the displacement field is governed by

$$\frac{\partial}{\partial y}\left(U_s\sin\phi\, b-D_T\frac{\partial b}{\partial y}\right)+\frac{\partial}{\partial\phi}\left(\Omega b-D_R\frac{\partial b}{\partial\phi}\right)=\left(\Omega^{\mathrm{eff}}-\Omega\right)g+2D_R\frac{\partial g}{\partial\phi}. \tag{2.19}$$

The angular velocity due to the flow is $\Omega=U_f y/H^2$. The conservation conditions are $\left\langle\int g(y,\phi)\mathrm{d}y\right\rangle=1$ and $\left\langle\int b(y,\phi)\mathrm{d}y\right\rangle=0$.

2.4. *Dimensionless equations*

To make the equations dimensionless, we scale length by the channel half-width H and time by the diffusive timescale $\tau_D=H^2/D_T$. Denoting dimensionless variables by

an overhead bar, we introduce the following variables,

$$\bar{y} = \frac{y}{H}, \tag{2.20a}$$
$$\bar{\Omega}^{\mathrm{eff}} = \Omega^{\mathrm{eff}}\tau_D \tag{2.20b}$$
$$\bar{D}_R^{\mathrm{eff}} = D_R^{\mathrm{eff}}\tau_D, \tag{2.20c}$$
$$\bar{g} = gH, \tag{2.20d}$$
$$\bar{b} = bH. \tag{2.20e}$$

Three dimensionless parameters dictate the behavior of the macrotransport dynamics. The first parameter is the swim Péclet number $Pe_s = U_s H/D_T$, which compares the relative importance of swim and translational diffusion. The second parameter is the flow Péclet number $Pe_f = U_f H/D_T$, which characterizes the relative dominance of fluid advection and translational diffusion. Lastly, $\gamma = H/\delta$ with $\delta = \sqrt{D_T\tau_R}$ and $\tau_R = 1/D_R$. Note that $\gamma^2 = \tau_D/\tau_R$, which compares the translational diffusion timescale τ_D to the reorientation time τ_R.

The dimensionless average field is governed by

$$\frac{\partial}{\partial\bar{y}}\left(Pe_s\sin\phi\,\bar{g} - \frac{\partial\bar{g}}{\partial\bar{y}}\right) + \frac{\partial}{\partial\phi}\left(Pe_f\,\bar{y}\,\bar{g} - \gamma^2\frac{\partial\bar{g}}{\partial\phi}\right) = 0. \tag{2.21}$$

The dimensionless displacement field is given by

$$\frac{\partial}{\partial\bar{y}}\left(Pe_s\sin\phi\,\bar{b} - \frac{\partial\bar{b}}{\partial\bar{y}}\right) + \frac{\partial}{\partial\phi}\left(Pe_f\,\bar{y}\,\bar{b} - \gamma^2\frac{\partial\bar{b}}{\partial\phi}\right) = \left(\bar{\Omega}^{\mathrm{eff}} - Pe_f\,\bar{y}\right)\bar{g} + 2\gamma^2\frac{\partial\bar{g}}{\partial\phi}. \tag{2.22}$$

We remark that the average field equation (2.21) is the same as that for the macrotransport of ABPs in linear space in Poiseuille flow (Peng & Brady 2020). Taking the zeroth orientational moment of $\bar{g}$ gives the number density, $\bar{n}(\bar{y}) = \int_0^{2\pi}\bar{g}(\bar{y},\phi)\mathrm{d}\phi$. From (2.12), we have

$$\bar{\Omega}^{\mathrm{eff}} = \frac{1}{2\pi}\int_0^{2\pi}\mathrm{d}\phi\int_{-1}^{1}\mathrm{d}\bar{y}\,Pe_f\,\bar{y}\,\bar{g} = \frac{1}{2\pi}\int_{-1}^{1}Pe_f\,\bar{y}\,\bar{n}(\bar{y})\mathrm{d}\bar{y} = 0, \tag{2.23}$$

where we have made use of the fact that $\bar{n}(-\bar{y}) = \bar{n}(\bar{y})$. As a result, the angular drift velocity vanishes in Poiseuille flow. Using (2.12), the dimensionless effective dispersion coefficient can be written as

$$\bar{D}_R^{\mathrm{eff}} = \gamma^2 - \left\langle\int_{-1}^{1}Pe_f\,\bar{y}\,\bar{b}\,\mathrm{d}\bar{y}\right\rangle. \tag{2.24}$$

The ratio between the dimensional dispersion coefficient and the bare diffusivity is given by

$$\frac{D_R^{\mathrm{eff}}}{D_R} = \frac{\bar{D}^{\mathrm{eff}}}{\gamma^2} = 1 - \frac{1}{\gamma^2}\left\langle\int_{-1}^{1}Pe_f\,\bar{y}\,\bar{b}\,\mathrm{d}\bar{y}\right\rangle. \tag{2.25}$$

To obtain the dispersion coefficient, we first need to solve (2.21). Using the solution to $\bar{g}$, we solve (2.22) and then calculate $\bar{D}_R^{\mathrm{eff}}$ using (2.24).

3. Results

3.1. *Weak-swimming asymptotic analysis*

Using asymptotic analysis, we consider the orientational dynamics in the weak-swimming limit characterized by $Pe_s \ll 1$. We pose regular expansions for all variables:

$$\bar{g} = \bar{g}_0 + Pe_s\,\bar{g}_1 + Pe_s^2\,\bar{g}_2 + O(Pe_s^3), \tag{3.1a}$$

$$\bar{b} = \bar{b}_0 + Pe_s\,\bar{b}_1 + Pe_s^2\,\bar{b}_2 + O(Pe_s^3), \tag{3.1b}$$

$$\bar{D}_R^{\mathrm{eff}} = \bar{D}_0^{\mathrm{eff}} + Pe_s\,\bar{D}_1^{\mathrm{eff}} + Pe_s^2\,\bar{D}_2^{\mathrm{eff}} + O(Pe_s^3). \tag{3.1c}$$

Henceforth, we shall use $\bar{D}^{\mathrm{eff}}$ as a shorthand for $\bar{D}_R^{\mathrm{eff}}$ for notational convenience. At $O(1)$, the particle is passive, i.e., not self-propelled.

3.1.1. *Passive Brownian particles*

At $O(1)$, the particle is a passive Brownian particle. The average field at this order is governed by

$$\frac{\partial}{\partial\bar{y}}\left(-\frac{\partial\bar{g}_0}{\partial\bar{y}}\right) + \frac{\partial}{\partial\phi}\left(Pe_f\,\bar{y}\,\bar{g}_0 - \gamma^2\frac{\partial\bar{g}_0}{\partial\phi}\right) = 0, \tag{3.2a}$$

$$-\frac{\partial\bar{g}_0}{\partial\bar{y}} = 0, \quad \bar{y} = \pm 1, \tag{3.2b}$$

$$\left\langle \int_{-1}^{1} \bar{g}_0 \mathrm{d}\bar{y} \right\rangle = 1, \tag{3.2c}$$

which has the solution $\bar{g}_0 = 1/2$. With this, the displacement field is governed by

$$\frac{\partial}{\partial\bar{y}}\left(-\frac{\partial\bar{b}_0}{\partial\bar{y}}\right) + \frac{\partial}{\partial\phi}\left(Pe_f\,\bar{y}\,\bar{b}_0 - \gamma^2\frac{\partial\bar{b}_0}{\partial\phi}\right) = -Pe_f\,\bar{y}\,\bar{g}_0, \tag{3.3a}$$

$$-\frac{\partial\bar{b}_0}{\partial\bar{y}} = 0, \quad \bar{y} = \pm 1, \tag{3.3b}$$

$$\left\langle \int_{-1}^{1} \bar{b}_0 \mathrm{d}\bar{y} \right\rangle = 0. \tag{3.3c}$$

The solution can be readily obtained as

$$\bar{b}_0 = \frac{1}{12} Pe_f\,\bar{y}\,\left(\bar{y}^2 - 3\right). \tag{3.4}$$

Using (2.12) and (3.4), we obtain the dispersion coefficient as

$$\bar{D}_0^{\mathrm{eff}} = \gamma^2 + \frac{2}{15} Pe_f^2. \tag{3.5}$$

In dimensional terms, we have

$$D_0^{\mathrm{eff}} = D_R + \frac{2}{15}\frac{U_f^2}{D_T}. \tag{3.6}$$

Scaling the dispersion coefficient by the bare diffusivity, we can write

$$\frac{D_0^{\mathrm{eff}}}{D_R} = 1 + \frac{2}{15}\frac{Pe_f^2}{\gamma^2}. \tag{3.7}$$

For a passive Brownian sphere obeying the Stokes-Einstein-Sutherland relation, we have $\zeta D_T = k_B T = \zeta_R D_R$, where ζ is the translational hydrodynamic drag coefficient, ζ_R is

the rotational drag coefficient, k_B is the Boltzmann constant, and T is the temperature. From this, we have $\gamma^2 = 3H^2/(4a^2)$, where a is the radius of the sphere, and we have used the drag coefficients of an isolated sphere in free space. We note that for active particles, Brownian motion can be of biological origin and the diffusion coefficients D_T and D_R are thus allowed to be independent parameters.

Just like the classical Taylor dispersion, for large Pe_f (strong flow), the dispersion coefficient D_0^{eff} scales quadratically with the flow speed. One may recover this scaling by considering the long-time random walk process. In the strong flow limit, the flow-induced angular velocity ($\Omega \sim U_f/H$) dominates the stochastic velocity due to Brownian motion, while the decorrelation time is given by the timescale τ_D. As particles migrate across streamlines, they experience a variation in their angular velocity. From a random walk perspective, we thus obtain $D_0^{\text{eff}} \sim \Omega^2 \tau_D = U_f^2/D_T$.

3.1.2. *First order*

At $O(Pe_s)$, the average field is governed by

$$\frac{\partial}{\partial \bar{y}}\left(-\frac{\partial \bar{g}_1}{\partial \bar{y}}\right) + \frac{\partial}{\partial \phi}\left(Pe_f\,\bar{y}\,\bar{g}_1 - \gamma^2 \frac{\partial \bar{g}_1}{\partial \phi}\right) = -\sin\phi\,\frac{\partial \bar{g}_0}{\partial \bar{y}}, \tag{3.8a}$$

$$\frac{\partial \bar{g}_1}{\partial \bar{y}} = \sin\phi\,\bar{g}_0, \quad \bar{y} = \pm 1, \tag{3.8b}$$

$$\left\langle \int_{-1}^{1} \bar{g}_1 \mathrm{d}\bar{y} \right\rangle = 0. \tag{3.8c}$$

We may guess a solution of the form

$$\bar{g}_1(\bar{y}, \phi) = A_1(\bar{y})\cos\phi + B_1(\bar{y})\sin\phi, \tag{3.9}$$

which leads to the following boundary value problems (BVPs):

$$-A_1'' + Pe_f\,\bar{y}\,B_1 + \gamma^2 A_1 = 0, \tag{3.10a}$$

$$-B_1'' - Pe_f\,\bar{y}\,A_1 + \gamma^2 B_1 = 0, \tag{3.10b}$$

$$A_1'(\pm 1) = 0, \quad B_1'(\pm 1) = \bar{g}_0, \tag{3.10c}$$

where the prime denotes differentiation with respect to $\bar{y}$.

The displacement field at this order is given by

$$-\frac{\partial^2 \bar{b}_1}{\partial \bar{y}^2} + \frac{\partial}{\partial \phi}\left(Pe_f\,\bar{y}\,\bar{b}_1 - \gamma^2 \frac{\partial \bar{b}_1}{\partial \phi}\right) = -\sin\phi\,\frac{\partial \bar{b}_0}{\partial \bar{y}} - Pe_f\,\bar{y}\,\bar{g}_1 + 2\gamma^2 \frac{\partial \bar{g}_1}{\partial \phi} \tag{3.11a}$$

$$\frac{\partial \bar{b}_1}{\partial \bar{y}} = \sin\phi\,\bar{b}_0, \quad \bar{y} = \pm 1, \tag{3.11b}$$

$$\left\langle \int_{-1}^{1} \bar{b}_1 \mathrm{d}\bar{y} \right\rangle = 0. \tag{3.11c}$$

Equation (3.11) admits a solution of the form

$$\bar{b}_1(\bar{y}, \phi) = A_2(\bar{y})\cos\phi + B_2(\bar{y})\sin\phi, \tag{3.12}$$

where the functions A_2 and B_2 are governed by

$$-A_2'' + Pe_f\,\bar{y} B_2 + \gamma^2 A_2 = -Pe_f\,\bar{y}\,A_1 + 2\gamma^2 B_1 \tag{3.13a}$$

$$-B_2'' - Pe_f\,\bar{y}\,A_2 + \gamma^2 B_2 = -\frac{\partial \bar{b}_0}{\partial \bar{y}} - Pe_f\,\bar{y}\,B_1 - 2\gamma^2 A_1 \tag{3.13b}$$

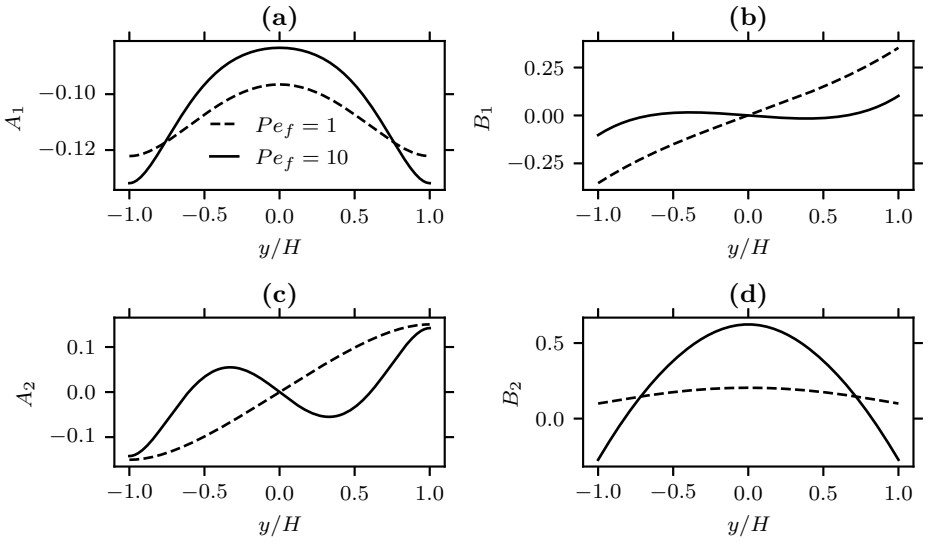

FIGURE 1. (a) Plot of A_1 as a function of $\bar{y}$ for $Pe_f = \{1, 10\}$. (b) Plot of B_1 as a function of $\bar{y}$ for $Pe_f = \{1, 10\}$. (c) Plot of A_2 as a function of $\bar{y}$ for $Pe_f = \{1, 10\}$. (d) Plot of B_2 as a function of $\bar{y}$ for $Pe_f = \{1, 10\}$. For all plots, $\gamma = 1$.

$$A_2'(\pm 1) = 0, \quad B_2'(\pm 1) = \bar{b}_0(\pm 1) = \mp \frac{1}{6} Pe_f. \tag{3.13c}$$

From (2.24) and (3.12), one can show that $\bar{D}_1^{\text{eff}}$ vanishes, i.e.,

$$\bar{D}_1^{\text{eff}} = -\left\langle \int_{-1}^{1} Pe_f \, \bar{y} \, \bar{b}_1 \, \mathrm{d}\bar{y} \right\rangle = 0. \tag{3.14}$$

Though the $O(Pe_s)$ fields $\bar{g}_1$ and $\bar{b}_1$ do not contribute to the effective dispersion, they provide forcing terms for the equations governing the fields at the next order. We solve the BVPs using a Chebyshev collocation method with 128 grid points. In figure 1, we plot the numerical solutions to A_1, B_1, A_2, and B_2 for different values of Pe_f for $\gamma = 1$.

3.1.3. *Second order*

At $O(Pe_s^2)$, the average field is governed by

$$-\frac{\partial^2 \bar{g}_2}{\partial \bar{y}^2} + \frac{\partial}{\partial \phi}\left(Pe_f \, \bar{y} \, \bar{g}_2 - \gamma^2 \frac{\partial \bar{g}_2}{\partial \phi} \right) = -\sin\phi \, \frac{\partial \bar{g}_1}{\partial \bar{y}}, \tag{3.15a}$$

$$\frac{\partial \bar{g}_2}{\partial \bar{y}} = \sin\phi \, \bar{g}_1, \quad \bar{y} = \pm 1, \tag{3.15b}$$

$$\left\langle \int_{-1}^{1} \bar{g}_2 \mathrm{d}\bar{y} \right\rangle = 0, \tag{3.15c}$$

which has a general solution of the form

$$\bar{g}_2(\bar{y}, \phi) = A_3(\bar{y}) + A_4(\bar{y}) \cos(2\phi) + B_3(\bar{y}) \sin(2\phi). \tag{3.16}$$

The displacement field at $O(Pe_s^2)$ is given by

$$-\frac{\partial^2 \bar{b}_2}{\partial \bar{y}^2} + \frac{\partial}{\partial \phi}\left(Pe_f \, \bar{y} \, \bar{b}_2 - \gamma^2 \frac{\partial \bar{b}_2}{\partial \phi} \right) = -\sin\phi \, \frac{\partial \bar{b}_1}{\partial \bar{y}} - Pe_f \, \bar{y} \, \bar{g}_2 + 2\gamma^2 \frac{\partial \bar{g}_2}{\partial \phi}, \tag{3.17a}$$

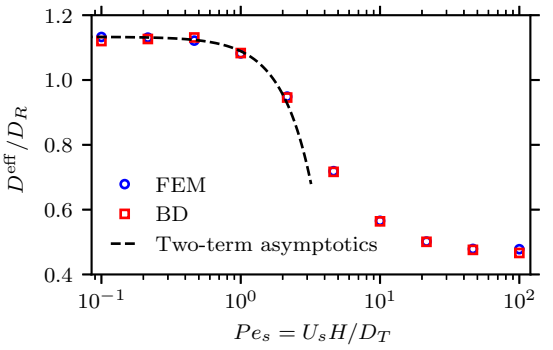

FIGURE 2. The effective rotational dispersion coefficient as a function of Pe_s with $\gamma = 1$ and $Pe_f = 1$. The circles are results obtained from solving the full macrotransport equations using FEM. The squares mark results from BD simulations. The two-term small Pe_s asymptotic solution in (3.23) is plotted in a dashed line.

$$\frac{\partial \bar{b}_2}{\partial \bar{y}} = \sin\phi\, \bar{b}_1, \quad \bar{y} = \pm 1, \tag{3.17b}$$

$$\left\langle \int_{-1}^{1} \bar{b}_2 \mathrm{d}\bar{y} \right\rangle = 0. \tag{3.17c}$$

Equation (3.17) admits a solution of the form

$$\bar{b}_2(\bar{y}, \phi) = A_5(\bar{y}) + A_6(\bar{y})\cos(2\phi) + B_4(\bar{y})\sin(2\phi). \tag{3.18}$$

Using (3.18), we write the dispersion coefficient as

$$\bar{D}_2^{\text{eff}} = -\int_{-1}^{1} Pe_f\, \bar{y}\, A_5(\bar{y})\, \mathrm{d}\bar{y}, \tag{3.19}$$

where A_5 is governed by

$$A_5'' = \frac{1}{2} B_2' + Pe_f\, \bar{y}\, A_3 \tag{3.20a}$$

$$A_5' = \frac{1}{2} B_2, \quad \bar{y} = \pm 1. \tag{3.20b}$$

The function A_3 is given by

$$2A_3'' = B_1', \tag{3.21a}$$

$$2A_3' = B_1, \quad \bar{y} = \pm 1. \tag{3.21b}$$

In addition, the following integral conditions need to be satisfied:

$$\int_{-1}^{1} A_3(\bar{y})\mathrm{d}\bar{y} = 0, \quad \text{and} \quad \int_{-1}^{1} A_5(\bar{y})\mathrm{d}\bar{y} = 0. \tag{3.22}$$

Because A_4, A_6, B_3, B_4 are not needed to calculate $\bar{D}_2^{\text{eff}}$, their solutions will not be discussed here.

We have shown that the first effect of swimming on the rotational dispersion appears

at $O(Pe_s^2)$. From (3.19), we have

$$\frac{D^{\text{eff}}}{D_R} = \frac{1}{\gamma^2}\left(\bar{D}_0^{\text{eff}} + Pe_s^2\bar{D}_2^{\text{eff}}\right) + o(Pe_s^2)$$
$$= 1 + \frac{2}{15}\frac{Pe_f^2}{\gamma^2} + Pe_s^2\frac{\bar{D}_2^{\text{eff}}}{\gamma^2} + o(Pe_s^2). \tag{3.23}$$

In figure 2, the two-term asymptotic solution given in (3.23) is plotted in a dashed line. The dispersion coefficient obtained from numerical solutions (see section 3.2) of the full macrotransport equations (2.21) and (2.22) is marked by circles. We also plot the results from BD simulations (squares). The two-term solution agrees well with both the numerical and the BD results in the small Pe_s regime. Compared to passive particles ($Pe_s \to 0$ in figure 2), activity suppresses the long-time rotational dispersion. In the small Pe_s expansion, this reduction means that $\bar{D}_2^{\text{eff}} < 0$. For all data shown in figure 2, $Pe_f = 1$ and $\gamma = 1$.

3.2. *Finite swim speeds*

For finite swim speeds, we solve the full macrotransport equations (2.21) and (2.22) using a finite element method implemented in `freefem++` (Hecht 2012). To validate our continuum theory, we compare the numerical results with those obtained by integrating the Langevin equations of motion using the Euler-Maruyama scheme. We calculate the rotational dispersion coefficient from the mean squared angular displacement at long times.

From a micromechanical perspective, the evolution of the position and orientation of an ABP is governed by the Langevin equations. In the absence of inertia, the equations are given by

$$\boldsymbol{0} = -\zeta\left(\frac{\mathrm{d}\boldsymbol{x}}{\mathrm{d}t} - \boldsymbol{u}_f\right) + \boldsymbol{F}^B + \boldsymbol{F}^S, \tag{3.24a}$$

$$\boldsymbol{0} = -\zeta_R\left(\frac{\mathrm{d}\boldsymbol{q}}{\mathrm{d}t} - \boldsymbol{\Omega}\times\boldsymbol{q}\right) + \boldsymbol{L}^B\times\boldsymbol{q}. \tag{3.24b}$$

In the above, ζ (ζ_R) is the translational (rotational) hydrodynamic drag coefficient, and $\boldsymbol{F}^S = \zeta U_s\boldsymbol{q}$ is the swim force. The Brownian force ($\boldsymbol{F}^B$) and torque ($\boldsymbol{L}^B$) satisfy white-noise statistics,

$$\left\langle\boldsymbol{F}^B\right\rangle_e = \boldsymbol{0}, \quad \left\langle\boldsymbol{F}^B(0)\boldsymbol{F}^B(t)\right\rangle_e = 2D_T\zeta^2\delta(t)\boldsymbol{I}, \tag{3.25a}$$

$$\left\langle\boldsymbol{L}^B\right\rangle_e = \boldsymbol{0}, \quad \left\langle\boldsymbol{L}^B(0)\boldsymbol{L}^B(t)\right\rangle_e = 2D_R\zeta_R^2\delta(t)\boldsymbol{I}, \tag{3.25b}$$

where $\delta(t)$ is the delta function, $\boldsymbol{I}$ is the identity tensor, and the angle brackets with a subscript 'e' denote the ensemble average over Brownian fluctuations. We note that for active particles the translational and rotational diffusion constants represent biological noises; as a result, they are treated as independent parameters.

In figure 3 we compare the results obtained from FEM (circles) with those from BD simulations (squares) as a function of Pe_f. The dashed line denotes the analytic solution when the swim speed is zero, i.e., $Pe_s = 0$ or $U_s = 0$. We observe good agreement between results from FEM and BD. For $Pe_s = 1$, activity is weak, and the dispersion coefficient follows closely that of the passive. For $Pe_s = 10$, we observe a non-monotonic variation of the dispersion as a function of Pe_f. In the limit $Pe_f \to 0$, we have $D^{\text{eff}} \to D_R$, or $D^{\text{eff}}/D_R \to 1$. In the strong flow limit, activity is overshadowed by the flow. As a result, D^{eff} asymptotes to the passive result as can be seen in figure 3. The initial decrease of

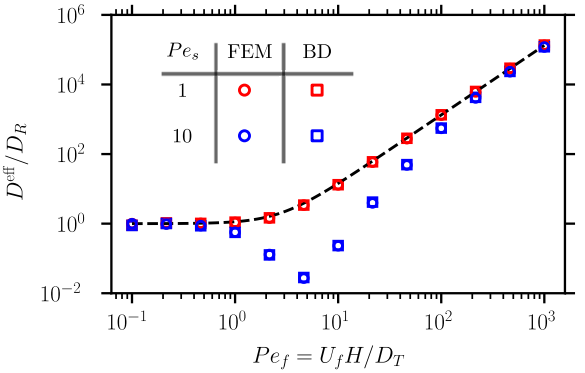

FIGURE 3. The effective rotational dispersion coefficient as a function of Pe_f for different values of Pe_s. For all results shown, $\gamma = 1$. Circles are results obtained from FEM solutions of the macrotransport equations and squares are from BD simulations. The dashed line denotes the analytic result for passive Brownian particles given in (3.7).

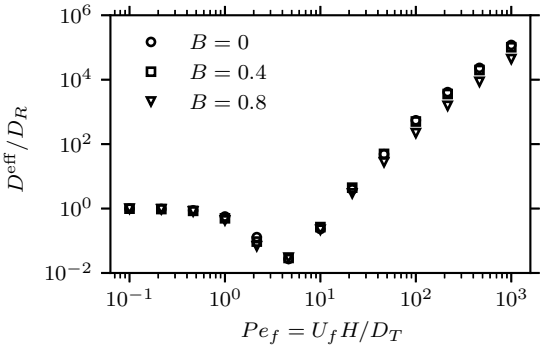

FIGURE 4. The effective rotational dispersion coefficient as a function of Pe_f for different particle shapes. For all results shown, $\gamma = 1$ and $Pe_s = 10$. All data are obtained from FEM.

the dispersion coefficient is a result of the swim-induced hindrance discussed in section 3.1.

3.3. *Non-spherical particles*

To probe the effect of particle shape on the long-time rotational dispersion, we consider active spheroids. We model the orientational dynamics of the spheroid in Poiseuille flow using Jeffery's equation (Jeffery 1922). In the Smoluchowski formulation, the only change is in the flow-induced angular velocity, which is given by $\boldsymbol{\Omega} = \boldsymbol{\omega}/2 + B\boldsymbol{q} \times (\boldsymbol{E} \cdot \boldsymbol{q})$. Here, $\boldsymbol{E} = \frac{1}{2}(\boldsymbol{\nabla u}_f + (\boldsymbol{\nabla u}_f)^{\intercal})$ is the rate-of-strain tensor, $B = (r^2 - 1)/(r^2 + 1) \in [0, 1)$ is the Bretherton constant (Bretherton 1962) that quantifies the non-spherical shape of the particle with r being the aspect ratio. For a sphere, $B = 0$. In the planar Poiseuille flow, the scalar angular velocity is given by

$$\Omega = \frac{U_f y}{H^2}\left[1 - B\cos(2\phi)\right], \quad -H \leqslant y \leqslant H. \tag{3.26}$$

In figure 4, we present the dispersion coefficient obtained from FEM as a function of Pe_f for different particle shapes. As shown in the figure, the dynamics is dominated by the contribution from the (ϕ independent) vorticity while the effect of the alignment from

the rate-of-strain tensor plays a less important role. From this, we see that the dispersion coefficient is insensitive to the variation of the particle shape. Such a weak dependence on the particle shape is also observed in the dispersion of ABPs in position space (Peng & Brady 2020).

4. Concluding remarks

In this paper, we have developed a generalized Taylor dispersion theory that characterizes the long-time orientational dynamics of an ABP in a background flow. We have showed that at long times the net orientational distribution of the ABP satisfies an advection diffusion equation, which allows us to define an average angular drift and an effective rotational dispersion coefficient. We emphasize that no particular assumptions about the geometry or flow have been made in deriving the macrotransport equations. That is, they can be applied to generic flows with or without confinement. For unbounded linear flows, we have shown that the equations reduce to those obtained by Peng (2024). We analyzed the macrotransport equations for a planar Poiseuille flow using a combination of asymptotic expansion and numerical solutions. The transport coefficients from the continuum theory agree with those obtained from BD simulations of the Langevin equations.

For passive Brownian spheres, a closed-form expression for the dispersion coefficient is obtained. The dispersion coefficient increases monotonically as a function of the flow speed and acquires a quadratic scaling with the flow speed in the strong flow limit. In the classical Taylor dispersion, the longitudinal dispersion coefficient along the channel also has a quadratic scaling. This universality can be understood by considering an effective random walk model that applies at long times. In both the translational (linear) and rotational dynamics, the long-time dispersion coefficient can be given by $\mathcal{U}^2\tau$, where $\mathcal{U}$ is a speed and τ is a decorrelation time associated with the random walk. For both longitudinal and rotational dispersion, the decorrelation time is given by the time it takes for the particle to diffuse across the channel ($\tau = \tau_D = H^2/D_T$), which allows the particle to access different linear and angular velocities from the flow. In the strong flow limit, the linear velocity associated with the random walk is given by U_f and the angular velocity is U_f/H. From this argument, we see that for both longitudinal and rotational dispersion, a quadratic scaling with the flow velocity is obtained.

It is also interesting to compare the rotational dispersion of passive Brownian particles in different flow fields. In an unbounded simple shear, prior studies (Leahy *et al.* 2013, 2015; Peng 2024) showed that $D^{\text{eff}}/D_R = O(1)$ for non-spherical particles in the strong shear limit. In simple shear, the angular velocity is spatially homogeneous. To achieve a flow-enhanced rotational dispersion, in simple shear a non-spherical shape is required. For a non-spherical particle, the angular velocity varies as a function of the local coordinate ϕ. In simple shear, the coupling between advection and diffusion results in a finite increase of the long-time dispersion compared to the bare diffusivity D_R. For Poiseuille flow, the enhancement is quadratic in Pe_f. This difference in scaling reveals that spatial variation of the fluid angular velocity gives rise to a much stronger enhancement to the long-time dispersion.

The dispersion behavior becomes even more interesting when one turns on activity. Compared to the case in which activity is absent (i.e., passive), through asymptotic analysis we showed that the swimming motion hinders rotational diffusion. As a result, for a fixed but finite activity, the dispersion coefficient is a non-monotonic function of the flow speed. The dispersion coefficient decreases before it increases and eventually asymptotes to that of passive particles in the strong flow limit. The transition from

decreasing to increasing occurs when $Pe_f \sim Pe_s$ or $U_f \sim U_s$ for a fixed γ. When $U_f \gg U_s$, activity is obscured by the flow and one recovers the passive result.

To conclude, we note that the coupling between flow-induced rotation, confinement, activity, and Brownian motion can give rise to nontrivial orientational dynamics. The results complement our theoretical understanding of the dynamics of active particles in Poiseuille flow. Because rotational motion can be used to probe the microrheology of a complex fluid (Cheng & Mason 2003; Andablo-Reyes *et al.* 2005; Schmiedeberg & Stark 2005; Wilhelm *et al.* 2003; Berret 2016), future work needs to study the effective orientational dynamics of a tracer particle in the presence of other particles.

Funding

This work is supported by the Faculty of Engineering at the University of Alberta.

Declaration of interests

The author reports no conflict of interest.

Author ORCID

Zhiwei Peng https://orcid.org/0000-0002-9486-2837

REFERENCES

Alonso-Matilla, Roberto, Chakrabarti, Brato & Saintillan, David 2019 Transport and dispersion of active particles in periodic porous media. *Phys. Rev. Fluids* **4** (4), 043101.

Andablo-Reyes, Efrén, Díaz-Leyva, Pedro & Arauz-Lara, José Luis 2005 Microrheology from rotational diffusion of colloidal particles. *Phys. Rev. Lett.* **94** (10), 106001.

Barakat, Joseph M. & Takatori, Sho C. 2023 Enhanced dispersion in an oscillating array of harmonic traps. *Phys. Rev. E* **107**, 014601.

Bearon, RN 2003 An extension of generalized Taylor dispersion in unbounded homogeneous shear flows to run-and-tumble chemotactic bacteria. *Phys. Fluids* **15** (6), 1552–1563.

Bearon, Rachel N, Bees, MA & Croze, OA 2012 Biased swimming cells do not disperse in pipes as tracers: a population model based on microscale behaviour. *Phys. Fluids* **24** (12).

Bees, Martin A & Croze, Ottavio A 2010 Dispersion of biased swimming micro-organisms in a fluid flowing through a tube. *Proc. R. Soc. A* **466** (2119), 2057–2077.

Berret, J-F 2016 Local viscoelasticity of living cells measured by rotational magnetic spectroscopy. *Nat. Commun.* **7** (1), 10134.

Brenner, Howard & Condiff, Duane W 1974 Transport mechanics in systems of orientable particles. iv. convective transport. *J. Colloid Interface Sci.* **47** (1), 199–264.

Brenner, Howard & Edwards, David A 1993 *Macrotransport processes*. Butterworth-Heinemann.

Bretherton, Francis P 1962 The motion of rigid particles in a shear flow at low Reynolds number. *J. Fluid Mech.* **14** (2), 284–304.

Cheng, Z & Mason, TG 2003 Rotational diffusion microrheology. *Phys. Rev. Lett.* **90** (1), 018304.

Doi, Masao & Edwards, Samuel Frederick 1988 *The theory of polymer dynamics*, , vol. 73. Oxford University Press.

Frankel, I & Brenner, Howard 1989 On the foundations of generalized Taylor dispersion theory. *J. Fluid Mech.* **204**, 97–119.

Hecht, Frédéric 2012 New development in freefem++. *J. Numer. Math.* **20** (3-4), 251–266.

Hill, NA & Bees, MA 2002 Taylor dispersion of gyrotactic swimming micro-organisms in a linear flow. *Phys. Fluids* **14** (8), 2598–2605.

Jeffery, George Barker 1922 The motion of ellipsoidal particles immersed in a viscous fluid. *Proc. R. Soc. A* **102** (715), 161–179.

Jiang, Weiquan & Chen, Guoqian 2019 Dispersion of active particles in confined unidirectional flows. *J. Fluid Mech.* **877**, 1–34.

Leahy, Brian D., Cheng, Xiang, Ong, Desmond C., Liddell-Watson, Chekesha & Cohen, Itai 2013 Enhancing rotational diffusion using oscillatory shear. *Phys. Rev. Lett.* **110**, 228301.

Leahy, Brian D., Koch, Donald L. & Cohen, Itai 2015 The effect of shear flow on the rotational diffusion of a single axisymmetric particle. *J. Fluid Mech.* **772**, 42–79.

Manela, A & Frankel, I 2003 Generalized Taylor dispersion in suspensions of gyrotactic swimming micro-organisms. *Journal of Fluid Mechanics* **490**, 99–127.

Peng, Zhiwei 2024 Rotational Taylor dispersion in linear flows. *arXiv preprint arXiv:2401.11603* .

Peng, Zhiwei & Brady, John F. 2020 Upstream swimming and Taylor dispersion of active Brownian particles. *Phys. Rev. Fluids* **5**, 073102.

Schmiedeberg, M & Stark, H 2005 One-bead microrheology with rotating particles. *Europhys. Lett.* **69** (4), 629.

Taylor, G. I. 1953 Dispersion of soluble matter in solvent flowing slowly through a tube. *Proc. R. Soc. A* **219** (1137), 186–203.

Trefethen, Lloyd N 2000 *Spectral methods in MATLAB*. SIAM.

Wilhelm, Claire, Browaeys, Julien, Ponton, Alain & Bacri, J-C 2003 Rotational magnetic particles microrheology: The Maxwellian case. *Phys. Rev. E* **67** (1), 011504.